Radiocarbon, Vol 62, Nr 4, 2020, p 919–937 DOI:10.1017/RDC.2020.16

SINGLE-YEAR GERMAN OAK AND CALIFORNIAN BRISTLECONE PINE ^{14}C DATA AT THE BEGINNING OF THE HALLSTATT PLATEAU FROM 856 BC TO 626 BC

Simon M Fahrni[1]* • John Southon[1] • Benjamin T Fuller[1,2] • Junghun Park[3] • Michael Friedrich[4] • Raimund Muscheler[5] • Lukas Wacker[6] • R E Taylor[7,8]†

[1]Department of Earth System Science, University of California, Irvine, CA, USA
[2]Department of Archaeology and Heritage Studies, School of Culture and Society, Aarhus University, Moesgård Allé 20, DK-8270, Højbjerg, Denmark
[3]Korea Institute of Geoscience and Mineral Resources, 124 Gwahang-no. Yuseong-gu, Daejeon 34132, Korea
[4]Institute of Botany, University of Hohenheim, Stuttgart, Germany
[5]Department of Geology, Lund University, Lund, Sweden
[6]Institute of Particle Physics, ETH, Zurich, Switzerland
[7]Department of Anthropology, University of California, Riverside, CA, USA
[8]Cotsen Institute of Archaeology, University of California, Los Angeles, CA, USA

ABSTRACT. As part of the ongoing effort to improve the Northern Hemisphere radiocarbon (^{14}C) calibration curve, this study investigates the period of 856 BC to 626 BC (2805–2575 yr BP) with a total of 403 single-year ^{14}C measurements. In this age range, IntCal13 was constructed largely from German and Irish oak as well as Californian bristlecone pine ^{14}C dates, with most samples measured with a 10-yr resolution. The new data presented here is the first atmospheric ^{14}C single-year record of the older end of the Hallstatt plateau based on an absolutely dated tree-ring chronology. The data helped reveal a major solar proton event (SPE) which caused a spike in the production rate of cosmogenic radionuclides around 2610/2609 BP. This production event is thought to have reached a magnitude similar to the 774/775 AD production event but has remained undetected due to averaging effects in the decadal calibration data. The record leading up to the 2610/2609 BP event reveals a 11-yr solar cycle with varying cyclicity. Features of the new data and the benefits of higher resolution calibration are discussed.

KEYWORDS: calibration, radiocarbon, IntCal, tree rings.

INTRODUCTION

The investigated period from 2805 to 2575 yr BP (856 BC to 626 BC) is of interest for both its significance as the beginning of the Hallstatt plateau, which masks the results of radiocarbon (^{14}C) dating between ~800 BC to ~400 BC and for its features of strongly decreasing atmospheric ^{14}C levels at 2625 BP and the subsequent production event at 2610/2609 BP. High-resolution, high-precision ^{14}C calibration data was therefore needed to improve this section of the ^{14}C calibration curve. Recent studies have investigated this section of interest on Japanese cedar tree-rings (Suzuki et al. 2010), on bristlecone pine tree-rings (Taylor and Southon 2013) and on sequoia (Jull et al. 2018). However, the cedar dates were obtained on a floating tree (no accurate dendro dates available), which had to be tied to the ^{14}C calibration curve through wiggle-matching (with an uncertainty of 8 years) and the bristlecone pine samples were measured at a temporal resolution of 10 years. The sequoia single-year study by Jull et al. (2018) spanned a rather short section before the Hallstatt plateau from 835 to 778 BC. Therefore, the current study provides the first single-year precision data obtained from a well-established dendrochronology on the pre- and early Hallstatt period.

Data from the current work has been previously published in parts by Park et al. (2017) and O'Hare et al. (2019). Data used in Park et al. (2017) is indicated with a superscript P and data used by O'Hare et al. (2019) is indicated with a superscript O in Tables 2 and 3, respectively. While Park et al. (2017) suggested a coronal mass ejection (CME) event for the 2610/2609 BP

†Deceased
*Corresponding author. Email: fahrni@ionplus.ch

^{14}C spike, O'Hare et al. (2019) analyzed NGRIP (North GReenland Ice core Project) ice core samples with sub-annual resolution for ^{10}Be and GRIP (GReenland Ice core Project) samples for ^{10}Be and ^{36}Cl. The inferred atmospheric production rates of cosmogenic radionuclides were found to be comparable to the most pronounced production event found thus far—the 774/775 AD event found by Miyake et al. (2012). The 774/775 AD event had been tentatively attributed to a solar origin by Melott and Thomas (2012). Mekhaldi et al. (2015) confirmed this hypothesis using ice core ^{10}Be and ^{36}Cl data. Similarly, the ratio of ^{10}Be and ^{36}Cl production rates of the 2610/2609 BP event suggest that the increased production rate had a solar origin (O'Hare et al. 2019). The main difference between the 774/775 AD event and the 2610/2609 BP event was the longer duration of the 2610/2609 BP event in the tree ring ^{14}C data, which has caused a less abrupt increase in the ^{14}C levels compared to the event of 774/775 AD. This prolonged duration and the smoothing of the decadal IntCal data (Reimer et al. 2013) led to a damped signal of the 2610/2609 BP production spike (Figure 4).

METHODS

Annual German oak samples from the 12,480-yr Hohenheim oak and pine tree-ring chronology (Friedrich et al. 2004) were obtained from the Institute of Botany, University of Hohenheim, Germany (whole-year and early-wood samples from three trees termed Oberhaid 15, Baunach 33, and Trieb 70 A). In addition, annual bristlecone pine samples from the White Mountains, California, USA (Ferguson 1969) were obtained from the Laboratory of Tree-Ring Research (LTRR), University of Arizona (whole-year samples from a tree termed CAM 143). The single-year tree rings were cleaned of obvious contamination and resin residues and cut into pieces of ~2 mg before weighing out to a total of ~25 mg of wood. The wood was then ABA (acid-base-acid) treated in 13-mm test tubes by consecutive washes in ~6 mL of 1 M HCl and 1 M NaOH solutions at 70°C for 30 min per step. After an initial acid wash, the wood pieces were treated 2 to 5 times with 1 M NaOH base solution until the solution showed only light discoloration. Upon the last base wash, the wood was put on acid one more time before washing it with Milli-Q water for 15 min at a time until a pH >6 was reached. The wood was then dried in a vacuum oven at 50°C for several hours until reaching baseline pressure.

In addition to the ABA treatment, a bleaching step was performed on a number of duplicate samples in order to compare the pure ABA treatment to bleaching of the wood to holocellulose. Therefore, up to 40 mg of wood were subjected to the treatment above and after the water washes the wood was bleached in 5 mL of a 0.5 M $NaClO_2$ and 0.5 M HCl solution at 70°C until the relatively dark wood had turned into almost white holocellulose (typically after 20–30 min). Upon complete bleaching, the holocellulose was washed with Milli-Q water for 30 min at 70°C repeatedly until a pH >6 was reached. These samples were then dried in a heating block at 70°C without vacuum as previous findings had indicated that the holocellulose was more prone to possible contamination in the vacuum oven than the ABA-only treated wood samples. All dried samples were capped with Fisher TainerTop closures for storage until further use.

For ^{14}C measurements, wood and holocellulose pieces of ~2.2 mg were combusted in quartz tubes (12.5 cm long, 4 mm I.D.) with ~60 mg prebaked CuO at 900°C for 3 hr. Upon cracking the quartz tubes in a vacuum line, the produced CO_2 was released and water from the oxidation was trapped in a dry ice slush trap. CO_2 was cryogenically transferred to graphitization reactors (Santos et al. 2007) and reduced over 5–6.5 mg iron powder with stoichiometric amounts of H_2.

https://doi.org/10.1017/RDC.2020.16 Published online by Cambridge University Press

The resulting iron/graphite mixture was then pressed in aluminum cathodes and measured by accelerator mass spectrometry (AMS) at the Keck Carbon Cycle AMS facility.

RESULTS AND DISCUSSION

Both a Wilcoxon signed-rank test and t-test showed no significant difference in treatments between the ABA and ABA bleach treated samples (n=8 data pairs). This finding was expected as the age range of the investigated wood samples was much younger than the ancient Kauri samples that Southon and Magana (2010) had found to be contaminated with traces of modern carbon. Upon this initial finding, all wood was prepared with ABA treatment only, as described in the Methods section.

The new single-year resolved data from this study is shown in Figure 1 (plotted as $\Delta^{14}C$, which denotes the relative deviation from a standard after correction for decay and isotopic fractionation) and Figure 2 (plotted as ^{14}C years) against calendar years. The data is also presented in Tables 1–4 in the appendix of this publication. It should be noted that two obvious outliers were not reproducible through remeasurement: the data points at 2724 BP (775 BC) and 2730 BP (781 BC) were off by more than 5-σ and 7-σ, respectively (Baunach 33 data, Table 1). Remeasurement confirmed that these two data points had been off, but the reason for these outliers remains obscure. The two outliers were not considered in the wavelet analysis or in any further discussion and are only shown for completeness.

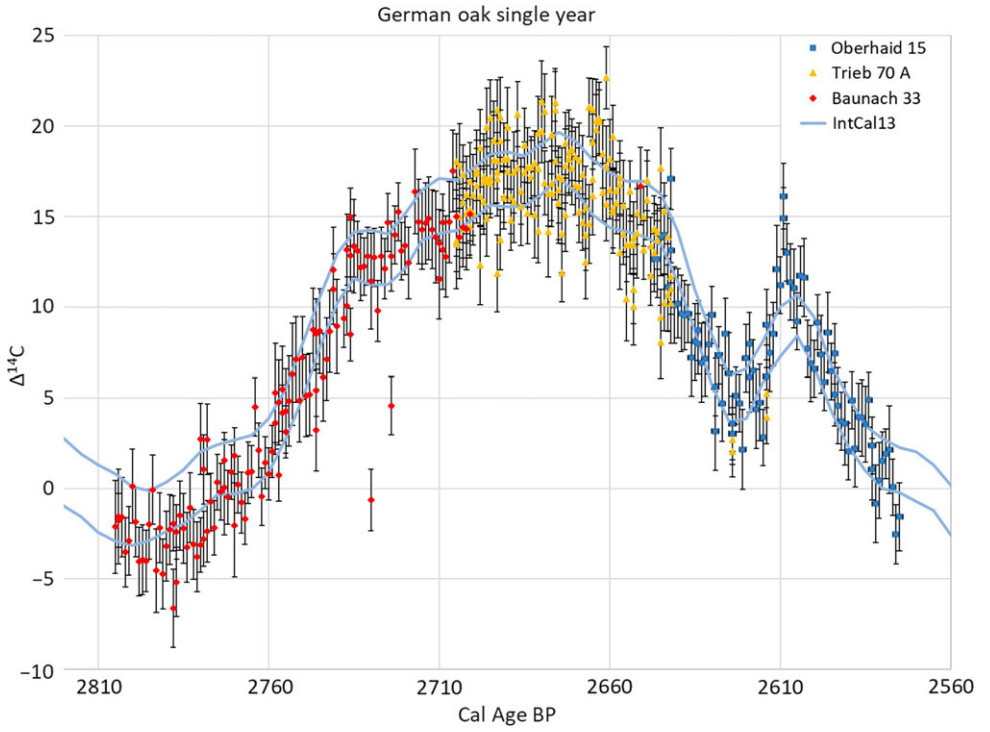

Figure 1 Results plotted as $\Delta^{14}C$ values, with their associated 1-σ errors. The IntCal13 1-σ error band is shown in light blue for comparison. The two outliers at 2724 BP and 2730 BP are included for completeness.

https://doi.org/10.1017/RDC.2020.16 Published online by Cambridge University Press

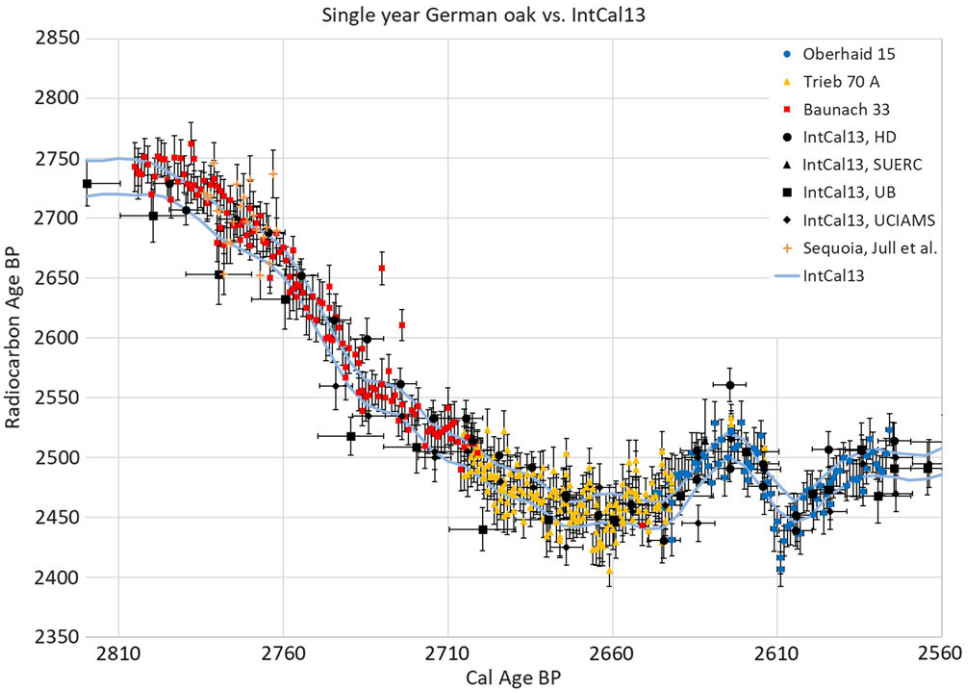

Figure 2 Results plotted as ^{14}C ages, with their associated 1-σ errors. The current IntCal13 1-σ error band is shown in light blue and the underlying datasets with their age spans and errors are shown grouped by ^{14}C lab codes. The two outliers at 2724 BP and 2730 BP are included for completeness.

Upon measurement, doubts on the correctness of the bristlecone pine dendro data emerged as it is unclear to this date, whether the dendro dates had been correctly converted to "years BC". Therefore, the bristlecone pine dendro ages are not certain to the exact year but may in fact need to be shifted by 1 calendar year. For example, a ^{14}C date now shown at 2610 BP might in fact belong to the year 2611 BP. While the accuracy and precision of the ^{14}C data are not affected by this potential shift in dendro dating, the new single-year bristlecone pine data will not go into IntCal20 for this reason. The Californian bristlecone data is, therefore, only plotted in Figure 4 for comparison and Table 4 indicates the alternative placement of the Californian bristlecone dates with calendar years in parentheses. The German oak data, on the other hand, has been submitted to IntCal and should become part of the data underlying IntCal20.

The new data generally confirms the existing IntCal13 curve but the following features are noted when comparing ^{14}C ages of Figure 2 to IntCal13: In the oldest part of the curve from 2805 BP until 2760 BP, the newly measured data is on average ca. 10 years older than the IntCal13 mean value. This is again the case around 2710 BP before the Trieb 70 A data displays more scatter than the previous section of Baunach 33. A feature around 2665 BP indicates additional fine structure that is not recognized by IntCal13. At around 2640 BP, the new data obtained from Baunach 33 and Oberhaid 15 trees again show slightly older ^{14}C ages than indicated by IntCal13. Finally, the increase in ^{14}C production at 2609 BP appears as a sharp drop in Figure 2 (peak in Figure 1) and is much sharper and more pronounced than in the IntCal13 data. This event has been compared to the 774/775 AD and 993/994

https://doi.org/10.1017/RDC.2020.16 Published online by Cambridge University Press

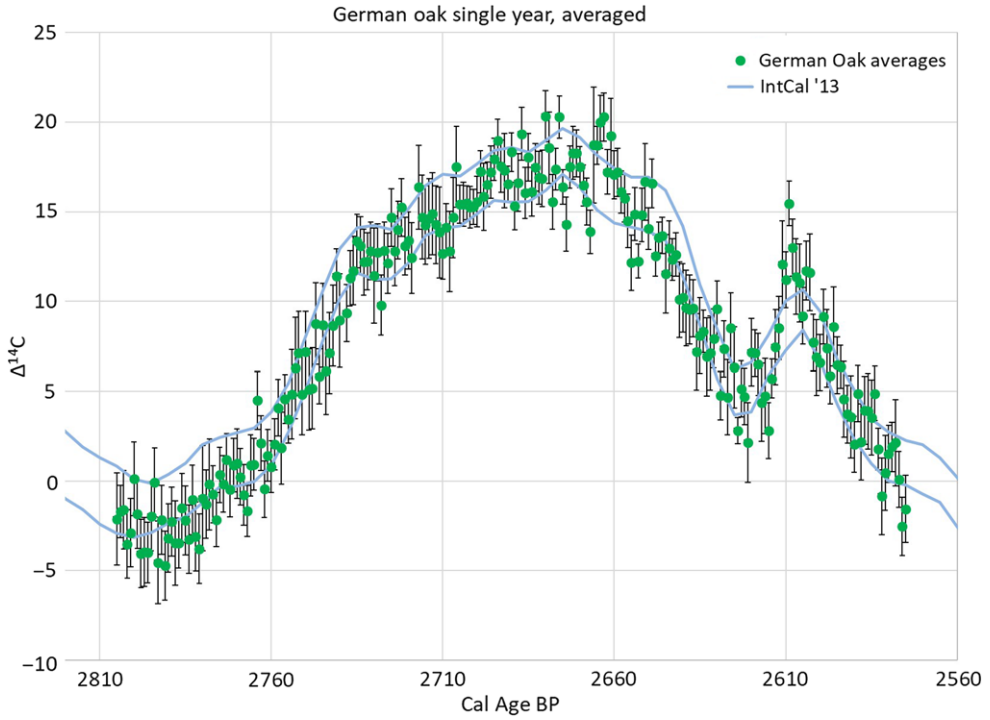

Figure 3 German oak dates, error-weighted averages. Errors were calculated as standard errors/reduced errors (larger value used).

AD events discovered by Miyake et al. (2012, 2013). While the $\Delta^{14}C$ peak starts as early as 2611 BP in ^{10}Be (O'Hare et al. 2019: supplemental information), it reaches its maximum around 2609 BP in ^{14}C. However, the ice core time scale was independently synchronized to tree ring ^{14}C with 1-σ uncertainties on the order of 2–3 yr (Adolphi and Muscheler 2016). Remeasurement of the ^{14}C peak may help to determine its exact shape and could lead to a more precise synchronization of the time scales.

Figure 2 compares the new single-year data to IntCal13 data (Reimer et al. 2013). IntCal13 is largely based on 10-year resolved German and Irish oak as well as Californian bristlecone pine data, which has been synthesized to a 5-yr resolved calibration curve in this age range. When considering the underlying data of IntCal13, it becomes clear why the 2610/2609 BP event's magnitude and exact timing had remained unresolved: While smoothing of the construction of IntCal may have damped the signal of the curve in certain spots, it is largely through the averaging of the decadal data that the 2610/2609 BP event was masked. It is therefore clear that fast changes in atmospheric ^{14}C levels, such as the ones stemming from extreme radionuclide production events, may only be seen at high temporal resolution. The trend towards covering larger sections of the calibration curve with single-year data is therefore important in the discovery of fast (production) events. A compilation of averaged values from all repetition measurements of the new German oak data is displayed in Figure 3 for more clarity. Both outlier values at 2724 BP and 2730 BP have been excluded from these averages.

https://doi.org/10.1017/RDC.2020.16 Published online by Cambridge University Press

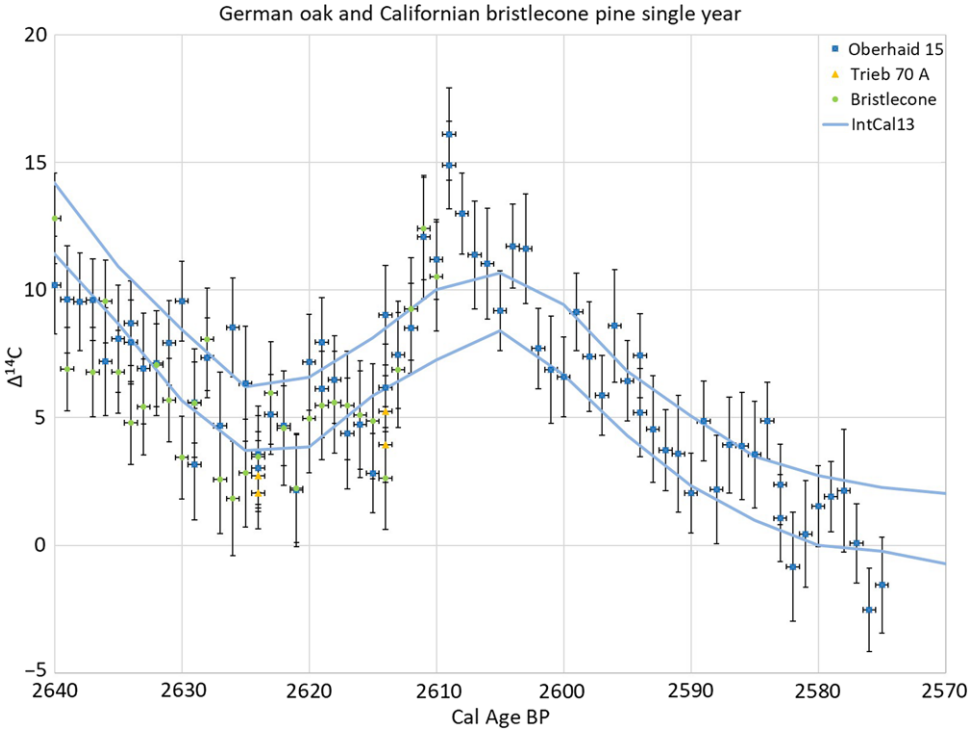

Figure 4 Detail view around the 2610/2609 BP event, including the new single-year German oak and the Californian bristlecone pine data.

A detailed view of the section from 2640 to 2570 BP is shown in Figure 4, where the Californian bristlecone pine data is included. Despite the uncertainty of the correctness of the absolute dendro dates (year zero problem), there is a striking similarity of the ^{14}C dates leading up to the 2610/2609 BP peak and it appears that the dendro dates are in fact correct to the exact year.

A problem in the conversion from Cal age BP or math BC to "regular" BC appears to have occurred during the preparation of Figure 3 in Park et al. (2017) as there is a shift of 1 calendar year compared to the dates reported here. The peak has been correctly called "660 BC" throughout Park et al. (2017) and only their Figure 3 shows the peak at 659 BC that should in fact occur at 660 BC (2609 BP). All findings of the Park et al. 2017 publication remain, therefore, intact but this discrepancy should be mentioned here for clarity and consistency.

With annual ^{14}C data one could expect to see the solar 11-yr cycle as discussed by Stuiver and Braziunas (1993) for annually resolved data from 1510 to 1954 AD. Such solar cycles have also been observed during periods of reduced production rates such as the period just before the 774/775 AD event (e.g. Park et al. 2017).

A wavelet analysis of the new German oak data does not show significant 11-yr cyclicity at the beginning of the Hallstatt plateau (Figure 5). However, band-pass filtering the data within a

https://doi.org/10.1017/RDC.2020.16 Published online by Cambridge University Press

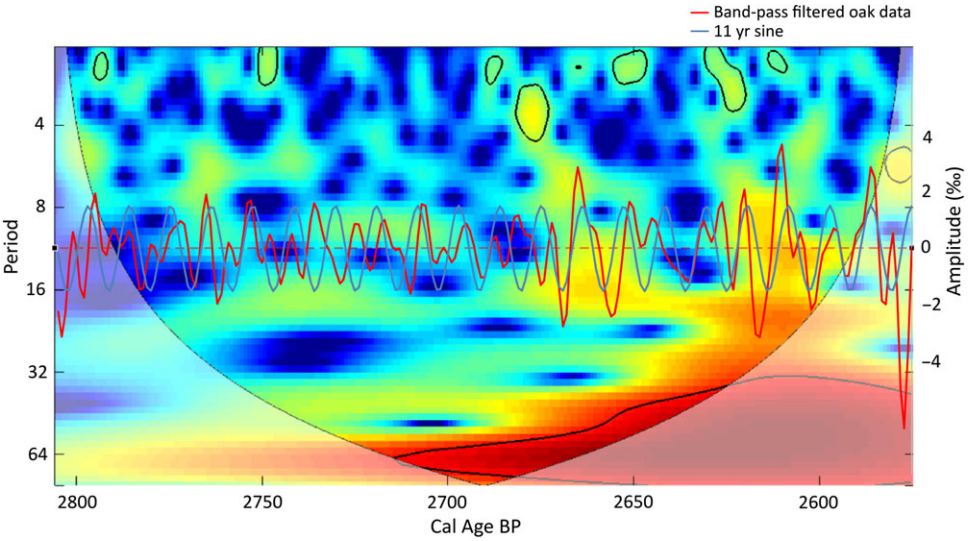

Figure 5 Wavelet analysis of the averaged German oak samples from Figure 3 calculated using the MATLAB packages of Grinsted et al. (2004) and Torrence and Compo (1998). The dotted line indicates the 11-yr periodicity and the areas outlined with solid lines indicate significant cycles detected with the wavelet analysis (Grinsted et al. 2004). An overlay of a band-pass filtered curve of the data from Figure 3 (red) and an artificial 11.1 year sine curve (blue) have been added for comparison. (Please see electronic version for color figures.)

frequency range from 1/5 yr^{-1} to 1/20 yr^{-1} does display a cyclicity, which appears to be more pronounced after 2675 BP, where amplitudes pick up and are better in phase with an (artificially added) 11.1 year sinusoidal signal (Figure 5). The band-pass filtered data was compared to band-pass filtered random (white noise) data to distinguish any signal from a filtering artifact. The analyzed cyclicity is consistent with a 0.8‰ amplitude and varying periodicity. Hence, this additional analysis yields smaller amplitudes than what the curve in Figure 5 suggests and artifacts of the band-pass filtering have to be taken into consideration when estimating amplitudes. The variation in periodicities explains the weak features in the wavelet analysis of Figure 5. It seems therefore, that the solar cycle exists even during the early Hallstatt plateau but is more dynamic than during other times. The exact causes of this higher variability in the signal are not understood at this time. The additional complexity in the data leading up to the solar proton event could be caused in part by the significantly elevated ^{14}C production rates, which may have counteracted the solar modulation effect on ^{14}C: if e.g. the event with increased production occurred during a solar cycle maximum (with increased galactic cosmic ray shielding, i.e. decreased production) it could mask the solar 11-yr cycle in the ^{14}C data.

CONCLUSION

New single-year ^{14}C data at the beginning of the Hallstatt plateau was obtained from German oak (early-wood and whole-year) and from Californian bristlecone pine (whole-year). This is the first atmospheric ^{14}C single-year record of the older end of the Hallstatt plateau based on an absolutely dated tree-ring chronology.

https://doi.org/10.1017/RDC.2020.16 Published online by Cambridge University Press

The data presented here generally matches and confirms the existing IntCal13 data, but adds some important details and more pronounced short-term features at 2665 BP and at 2610/2609 BP. Additional high resolution single-year measurements are needed to improve the IntCal data and to detect other short-term production events that can take place within a few years, as these events can remain undetected with decadal data. Despite the constant improvement of the IntCal data, the resolution of the underlying data must be considered when accurate ^{14}C dating is of the essence. The solar cyclicity appears to be highly dynamic with varying cycle lengths over the entire analyzed period and further analysis may be needed to better understand the underlying causes of this observation. Finally, there is some doubt on the exact calendar age of the Californian bristlecone pine data (uncertainty of 1 calendar year) and the new bristlecone pine data will therefore not be part of IntCal20. The new German oak data on the other hand has been submitted for IntCal20 and will add much needed higher resolution to the IntCal data from 856 BC to 626 BC (2805 to 2575 yr BP).

ACKNOWLEDGMENTS

The authors would like to thank Dr. Paul Creasman of the Laboratory of Tree-Ring Research (LTRR), University of Arizona, for his collaboration in obtaining the tree-ring-dated samples from the LTRR collections. Portions of this research were supported by the Gabrielle O. Vierra Memorial Fund and the W.M. Keck foundation and UCI. This paper is dedicated to our late colleague Erv Taylor, whose dating studies of archaeological material associated with the sack of the Assyrian capital of Nineveh in 612 BC (Taylor et al. 2010) led directly to our interest in the unusual character of the radiocarbon calibration curve at the start of the Hallstatt Plateau.

REFERENCES

Adolphi F, Muscheler R. 2016. Synchronizing the Greenland ice core and radiocarbon timescales over the Holocene – Bayesian wiggle-matching of cosmogenic radionuclide records. Clim. Past 12:15–30.

Ferguson CW. 1969. A 7104-year annual tree-ring chronology for bristlecone pine, pinus aristate, from the white mountains, California. Tree-Ring Bulletin 29(3-4):3–29.

Friedrich M, Remmele S, Kromer B, Hofmann J, Spurk M, Kaiser KF, Orcel C, Küppers M. 2004. The 12,460-year Hohenheim oak and pine tree-ring chronology from central Europe—a unique annual record for radiocarbon calibration and paleoenvironment reconstructions. Radiocarbon 46(3):1111–1122.

Grinsted A, Moore JC, Jevrejeva S. 2004. Application of the cross wavelet transform and wavelet coherence to geophysical time series: Nonlin. Processes Geophys., 11:561–566.

Jull AJT, Panyushkina I, Miyake F, Masuda K, Nakamura T, Mitsutani T, Lange TE, Cruz RJ, Baisan C, Janovics R, Varga T, Molnár M. 2018. More rapid ^{14}C excursions in the tree-ring record: a record of different kind of solar activity at about 800 BC? Radiocarbon 60(4): 1237–1248.

Melott AL, Thomas BC. 2012. Causes of an AD 774–775 ^{14}C increase. Nature 491:E1.

Mekhaldi F, Muscheler R, Adolphi F, Aldahan A, Beer J, McConnell JR, Possnert G, Sigl M, Svensson A, Synal H-A, Welten KC, Woodruff TE. 2015. Multiradionuclide evidence for the solar origin of the cosmic-ray events of AD 774/5 and 993/4. Nature Communications 6:8611.

Miyake F, Nagaya K, Masuda K, Nakamura T. 2012. A signature of cosmic-ray increase in AD 774–775 from tree rings in Japan. Nature 486:240–242.

Miyake F, Masuda K, Nakamura T. 2013. Another rapid event in the carbon-14 content of tree rings. Nature Communications 4:1748.

O'Hare P, Mekhaldi F, Adolphi F, Raisbeck G, Aldahan A, Anderberg E, Beer J, Christl M, Fahrni S, Synal H-A, Park J, Possnert G, Southon J, Bard E, ASTER team, Muscheler R. 2019. Multiradionuclide evidence for an extreme solar proton event around 2610 BP (~660 BC). PNAS 116(13):5961–5966.

Park J, Southon J, Fahrni S, Creasman PP, Mewaldt R. 2017. Relationship between solar activity and delta C-14 peaks in AD 775, AD 994, and 660 BC. Radiocarbon 53(4):1147–1156.

https://doi.org/10.1017/RDC.2020.16 Published online by Cambridge University Press

Reimer PJ, Bard E, Bayliss A, Beck JW, Blackwell PG, Bronk Ramsey C, Buck CE, Cheng H, Edwards RL, Friedrich M, Grootes PM, Guilderson TP, Haflidason H, Hajdas I, Hatte C, Heaton TJ, Hoffman DL, Hogg AG, Hughen KA, Kaiser KF, Kromer B, Manning SW, Niu M, Reimer RW, Richards DA, Scott EM, Southon JR, Staff RA, Turney CSM, van der Plicht J. 2013. IntCal13 and Marine13 radiocarbon age calibration curves 0–50,000 years cal BP. Radiocarbon 55(4):1869–1887.

Santos G, Moore R, Southon J, Griffin S, Hinger E, Zhang D. (2007). AMS ^{14}C sample preparation at the KCCAMS/UCI facility: Status report and performance of small samples. Radiocarbon 49(2):255–269.

Southon J, Magana AL. 2010. A comparison of cellulose extraction and ABA pretreatment methods for AMS ^{14}C dating of ancient wood. Radiocarbon 52(3):1371–1379.

Stuiver M, Braziunas TF. 1993. Sun, ocean, climate and atmospheric $^{14}CO_2$: an evaluation of causal and spectral relationships. The Holocene 3(4):289–305.

Suzuki K, Sakurai H, Takahashi Y, Sato T, Gunji S, Tokanai F, Matsuzaki H, Tsuchiya YS. 2010. Precise comparison of ^{14}C ages from choukai jindai cedar with IntCal04 raw data. Radiocarbon 52(4):1599–1609.

Taylor RE, Beaumont WC, Southon J, Stronach D, Pickworth D. 2010. Alternative explanations for anomalous ^{14}C ages on human skeletons associated with the 612 BCE destruction of Nineveh. Radiocarbon 52(2-3):372–382.

Taylor RE, Southon J. 2013. Reviewing the mid-first Millennium BC ^{14}C "warp" using ^{14}C/bristlecone pine data. Nuclear Instruments and Methods in Physics Research B 294:440–443.

Torrence C, Compo GP. 1998. A practical guide to wavelet analysis. Bulletin of the American Meteorological Society 79:61–78.

https://doi.org/10.1017/RDC.2020.16 Published online by Cambridge University Press

APPENDIX

Table 1 Single-year dates from Baunach, Tree 33, early-wood. Crossed out, asterisked samples were found to be outliers.

Year (yr BC)	^{14}C age (yr BP)	^{14}C age error (yr BP)	Δ^{14}C (‰)	Δ^{14}C error (‰)	UCIAMS #
856	2743	21	–2.1	2.6	147756
855	2737	21	–1.6	2.6	147755
855	2739	12	–1.8	1.5	161489
854	2736	18	–1.6	2.2	161953
853	2751	15	–3.5	1.9	161952
852	2745	15	–2.9	1.9	161951
851	2720	16	0.1	2.0	161950
850	2735	15	–1.9	1.9	161949
849	2751	15	–4.0	1.9	161948
848	2750	16	–4.0	1.9	161947
847	2749	14	–4.0	1.7	161946
846	2732	15	–2.0	1.9	161943
845	2715	15	–0.1	1.9	161942
844	2751	19	–4.5	2.3	161941
843	2730	16	–2.2	1.9	161940
842	2750	16	–4.7	1.9	161939
841	2737	15	–3.2	1.9	161938
840	2728	16	–2.3	1.9	161937
839	2725	12	–1.9	1.5	161488
839	2762	17	–6.6	2.2	161936
838	2727	12	–2.4	1.5	161487
838	2750	15	–5.2	1.9	161935
837	2719	15	–1.5	1.9	161934
836	2724	15	–2.2	1.9	161931
835	2731	15	–3.3	1.9	161930
834	2713	16	–1.1	1.9	161929
833	2728	16	–3.1	1.9	161928
832	2733	16	–3.8	1.9	161927
831	2727	12	–3.1	1.5	161486
831	2679	16	2.7	2.0	161926
830	2723	12	–2.8	1.5	161485
830	2692	15	1.1	1.9	161925
829	2718	14	–2.4	1.7	161484
829	2678	16	2.7	2.0	161924
828	2704	13	–0.7	1.6	161482
827	2715	12	–2.2	1.5	161481
826	2694	12	0.3	1.5	161480
825	2697	13	–0.2	1.6	161479
824	2694	21	0.1	2.6	147753
824	2682	12	1.6	1.5	161478
823	2697	12	–0.5	1.5	161477

https://doi.org/10.1017/RDC.2020.16 Published online by Cambridge University Press

822	2685	12	0.9	1.5	161476
821	2708	23	–2.1	2.8	147752
821	2677	12	1.8	1.5	161475
820	2689	13	0.2	1.6	161474
819	2696	14	–0.8	1.7	161473
818	2702	12	–1.7	1.4	161470
817	2681	14	0.9	1.7	161469
816	2679	12	0.9	1.4	161468
815	2650	13	4.5	1.6	161467
814	2668	12	2.1	1.5	161466
813	2687	13	–0.5	1.6	161465
812	2671	12	1.4	1.4	161464
811	2675	12	0.8	1.4	161463
810	2664	12	2.0	1.4	161462
809	2638	22	5.3	2.7	136725
809	2651	14	3.6	1.7	161460
808	2641	19	4.7	2.3	136724
808	2673	12	0.7	1.4	161459
807	2634	19	5.5	2.3	136723
807	2645	12	4.2	1.5	161458
806	2643	19	4.3	2.3	136722
806	2652	12	3.1	1.4	161457
805	2637	20	4.8	2.5	136721
804	2625	22	6.3	2.8	136720
803	2617	19	7.1	2.3	136719
802	2634	18	4.8	2.3	136718
801	2615	18	7.2	2.3	136717
800	2630	18	5.1	2.3	136716
799	2629	18	5.2	2.3	136714
798	2599	18	8.8	2.3	136713
797	2643	18	3.2	2.3	136712
797	2625	12	5.4	1.4	161456
797	2600	15	8.5	1.9	161921
796	2598	19	8.7	2.3	136711
795	2617	19	6.1	2.4	136710
794	2608	18	7.1	2.3	136709
793	2595	18	8.7	2.3	136708
792	2567	19	12.1	2.3	136707
792	2576	15	11.0	1.9	161920
791	2591	21	8.9	2.6	136706
789	2586	13	9.4	1.6	136378
788	2579	13	10.1	1.6	136377
788	2555	16	13.2	2.0	161919
787	2539	13	15.0	1.6	136376
787	2591	12	8.5	1.4	161453
787	2556	16	12.8	2.0	161918
786	2551	13	13.4	1.7	136375
786	2551	20	13.4	2.6	161917
785	2552	13	13.1	1.6	136374

https://doi.org/10.1017/RDC.2020.16 Published online by Cambridge University Press

Table 1 (*Continued*)

Year (yr BC)	^{14}C age (yr BP)	^{14}C age error (yr BP)	Δ^{14}C (‰)	Δ^{14}C error (‰)	UCIAMS #
784	2558	15	12.2	1.8	136373
783	2557	13	12.2	1.6	136372
782	2551	13	12.8	1.6	136371
~~781~~	~~2658~~	~~14~~	~~−0.6~~	~~1.7~~	~~136370~~*
781	2561	21	11.4	2.7	147751
780	2550	13	12.7	1.6	136369
779	2573	13	9.8	1.7	136366
778	2547	13	12.8	1.6	136365
777	2552	13	12.1	1.7	136364
776	2531	13	14.7	1.6	136363
~~775~~	~~2610~~	~~13~~	~~4.6~~	~~1.6~~	~~136362~~*
775	2545	15	12.8	1.9	161956
774	2534	13	14.0	1.6	136361
773	2523	13	15.2	1.6	136360
772	2540	13	13.1	1.6	136359
771	2536	13	13.4	1.6	136358
770	2543	16	12.4	2.0	136357
768	2510	18	16.4	2.3	141758
767	2522	18	14.7	2.3	141757
766	2524	17	14.3	2.2	113427
765	2521	18	14.6	2.2	113426
764	2517	18	14.9	2.3	113425
763	2521	17	14.3	2.2	113424
762	2524	20	13.9	2.5	113423
761	2541	17	11.5	2.2	113422
761	2525	15	13.5	1.9	168493
760	2527	17	13.1	2.2	113421
760	2515	13	14.7	1.6	168503
759	2529	18	12.8	2.2	113420
758	2513	18	14.7	2.2	113419
757	2490	18	17.5	2.2	113418
756	2509	17	15.0	2.2	113417
755	2517	18	13.9	2.3	113416
754	2512	17	14.4	2.2	113415
753	2511	18	14.3	2.2	113414
752	2504	19	15.1	2.4	113412
702	2443	17	16.7	2.1	113411

https://doi.org/10.1017/RDC.2020.16 Published online by Cambridge University Press

Table 2 Single-year dates from Trieb, Tree 70a, early-wood. A compilation of samples marked with a superscript "P" have been used in the previously published work of Park et al. (2017) and samples marked with a superscript "O" have been used in the work published by O'Hare et al. (2019).

Year (yr BC)	^{14}C age (yr BP)	^{14}C age error (yr BP)	$\Delta^{14}C$ (‰)	$\Delta^{14}C$ error (‰)	UCIAMS #
756	2521	20	13.5	2.5	113410
756	2485	12	18.0	1.6	166622
756	2520	13	13.6	1.7	168502
755	2486	18	17.8	2.3	113409
755	2508	14	15.0	1.8	168492
754	2501	18	15.8	2.2	113408
754	2489	13	17.3	1.7	166621
754	2512	13	14.3	1.6	168501
753	2497	17	16.2	2.1	113407
753	2504	13	15.2	1.7	168491
752	2490	17	16.9	2.2	113406
752	2509	12	14.4	1.6	166620
752	2502	13	15.4	1.7	168500
751	2495	18	16.2	2.2	113405
751	2502	14	15.2	1.8	168490
750	2484	19	17.4	2.4	113404
750	2490	16	16.7	2.1	166299
750	2483	13	17.5	1.7	168499
749	2472	17	18.8	2.1	113403
749	2523	17	12.3	2.2	167109
749	2493	13	16.1	1.7	168489
748	2486	21	16.9	2.6	113402
748	2484	16	17.2	2.0	166298
748	2495	14	15.8	1.8	168498
747	2461	17	19.9	2.1	113401
747	2501	17	14.9	2.1	167108
747	2484	15	17.0	1.8	168488
746	2482	17	17.1	2.2	113400
746	2456	17	20.5	2.1	166297
746	2485	13	16.8	1.7	168497
745	2465	17	19.2	2.2	113399
745	2473	19	18.1	2.5	167107
745	2465	12	19.2	1.6	168487
744	2478	13	17.5	1.7	112855
744	2522	17	11.9	2.1	113398
744	2481	16	17.1	2.1	166296
744	2473	12	18.1	1.6	166619
744	2451	13	20.9	1.7	168496
743	2463	14	19.2	1.7	112854
743	2453	17	20.5	2.2	167106
743	2506	13	13.7	1.7	168486
742	2487	11	16.1	1.4	112853

https://doi.org/10.1017/RDC.2020.16 Published online by Cambridge University Press

Table 2 (*Continued*)

Year (yr BC)	^{14}C age (yr BP)	^{14}C age error (yr BP)	Δ^{14}C (‰)	Δ^{14}C error (‰)	UCIAMS #
742	2471	16	18.1	2.0	166295
742	2487	14	16.0	1.7	168495
741	2475	14	17.5	1.7	112852
741	2455	17	19.9	2.2	167105
741	2469	13	18.2	1.7	168485
740	2495	13	14.8	1.7	112851
740	2485	16	16.1	2.0	166294
739	2486	18	15.8	2.3	112850
739	2473	18	17.4	2.2	167104
738	2447	14	20.6	1.8	112849
738	2470	16	17.7	2.1	166293
737	2479	14	16.4	1.8	112848
737	2486	17	15.6	2.2	167103
736	2470	13	17.4	1.7	112847
736	2458	16	18.9	2.0	166292
735	2487	13	15.2	1.7	112846
735	2467	17	17.7	2.2	167102
734	2466	13	17.7	1.7	112845
734	2470	16	17.2	2.0	166291
733	2463	14	17.9	1.8	112844
733	2486	19	15.1	2.4	167101
732	2492	14	14.2	1.8	112843
732	2449	16	19.6	2.0	166019
732	2465	16	17.6	2.0	166030
731	2447	14	19.7	1.8	112842
731	2434	18	21.4	2.3	167097
730	2469	14	16.9	1.8	112841
730	2438	16	20.8	2.0	166288
729	2473	14	16.3	1.8	112840
729	2489	20	14.2	2.5	167096
728	2472	14	16.3	1.8	104806
728	2467	16	16.8	2.1	166017
728	2446	17	19.5	2.1	166027
727	2431	13	21.3	1.7	112838
727	2456	17	18.1	2.2	167095
727	2434	18	20.9	2.3	167117
726	2462	13	17.2	1.7	104805
726	2474	18	15.7	2.2	166018
726	2474	16	15.7	2.0	166029
726	2468	14	16.4	1.8	166618
725	2462	13	17.1	1.7	112837
725	2503	13	11.9	1.6	166632
725	2486	17	14.1	2.2	167116
724	2446	14	19.0	1.7	104804
724	2456	16	17.8	2.0	166016

https://doi.org/10.1017/RDC.2020.16 Published online by Cambridge University Press

724	2477	16	15.1	2.0	166026
723	2452	15	18.2	1.9	112836
723	2449	19	18.5	2.4	167094
722	2447	13	18.7	1.7	104803
722	2455	16	17.7	2.0	166287
721	2461	13	16.7	1.6	112835
721	2449	13	18.3	1.6	166631
720	2472	14	15.3	1.7	104802
720	2461	17	16.6	2.1	166015
720	2449	16	18.1	2.1	166025
719	2475	12	14.7	1.6	112834
719	2455	17	17.3	2.2	167093
718	2480	16	14.0	2.0	104801
718	2468	18	15.5	2.3	166028
718	2492	16	12.5	2.0	166286
717	2423	13	21.0	1.6	112833
717	2474	17	14.6	2.2	167115
716	2423	13	20.9	1.7	104800
716	2454	16	17.1	2.0	166014
716	2461	17	16.1	2.2	166024
716	2437	12	19.1	1.5	166616
715	2431	15	19.8	1.9	112832
715	2427	18	20.3	2.3	167092
714	2427	14	20.2	1.8	104799
714	2425	16	20.4	2.0	166285
713	2456	13	16.3	1.6	112831
713	2440	15	18.4	1.9	166630
712	2406	13	22.7	1.7	104798
712	2444	18	17.8	2.2	113430
712	2461	16	15.7	2.0	166013
711	2453	13	16.5	1.6	112830
711	2440	17	18.2	2.2	167091
710	2429	14	19.4	1.7	104797
710	2461	17	15.4	2.2	113429
710	2462	18	15.2	2.3	166284
709	2457	13	15.8	1.7	112829
709	2452	13	16.4	1.6	166629
708	2448	14	16.8	1.7	104796
708	2478	16	13.0	2.0	166012
708	2445	16	17.1	2.0	166023
707	2469	13	14.0	1.7	112828
707	2457	20	15.6	2.5	167090
706	2473	16	13.4	2.0	104795
706	2496	18	10.5	2.3	166283
705	2472	13	13.4	1.6	112827
705	2448	13	16.4	1.7	166628
704	2490	15	11.0	1.9	104469
704	2498	17	10.0	2.1	166011
704	2468	16	13.8	2.0	166022

https://doi.org/10.1017/RDC.2020.16 Published online by Cambridge University Press

Table 2 (*Continued*)

Year (yr BC)	^{14}C age (yr BP)	^{14}C age error (yr BP)	Δ^{14}C (‰)	Δ^{14}C error (‰)	UCIAMS #
704	2471	12	13.4	1.6	166615
703	2456	14	15.2	1.8	112826
703	2465	20	14.1	2.5	167089
701	2455	13	15.0	1.7	112825
701	2470	13	13.2	1.6	166627
700	2439	13	17.0	1.7	104468
700	2447	17	15.9	2.2	166282
699	2467	13	13.3	1.6	112824
699	2480	13	11.7	1.6	166633
698	2458	11	14.3	1.4	102857
698	2458	14	14.3	1.8	102858
698	2468	17	13.0	2.2	167114
697	2458	12	14.2	1.5	104467
697	2462	13	13.7	1.6	166626
696	2429	18	17.7	2.2	104466
696	2506	16	8.1	2.0	166281
696	2495	12	9.4	1.5	166617
695	2447	13	15.3	1.6	104465
695	2487	12	10.2	1.5	166623
694	2457	12	13.9	1.6	104464
694	2483	16	10.7	2.0	166280
693	2474	11	11.7	1.4	102859
693	2479	11	11.0	1.4	102860
693	2486	18	10.2	2.2	167113
675^{O}	2533	11	2.0	1.4	102861
675^{O}	2528	11	2.7	1.4	102862
665$^{P, O}$	2498	11	5.3	1.4	102863
665$^{P, O}$	2508	12	3.9	1.5	102864

Table 3 Single-year dates from Oberhaid, Tree 15, whole-year rings. A compilation of samples marked with a superscript "P" have been used in the previously published work of Park et al. (2017) and samples marked with a superscript "O" have been used in the work published by O'Hare et al. (2019).

Year (yr BC)	^{14}C age (yr BP)	^{14}C age error (yr BP)	Δ^{14}C (‰)	Δ^{14}C error (‰)	UCIAMS #
698	2471	11	12.7	1.4	102847
697	2470	17	12.6	2.1	103358
696	2459	17	13.9	2.2	103359
695	2458	17	14.0	2.2	103347
694	2480	19	11.1	2.4	103360
693	2463	14	13.1	1.8	100862
693	2431	13	17.1	1.7	100863

https://doi.org/10.1017/RDC.2020.16 Published online by Cambridge University Press

692	2485	17	10.1	2.1	103361
691	2484	15	10.2	1.9	102848
690[O]	2487	17	9.6	2.1	103362
689[O]	2487	15	9.5	1.9	102849
688[O]	2485	13	9.6	1.6	104463
687[O]	2504	17	7.2	2.1	103363
686[O]	2496	17	8.1	2.1	103364
685[O]	2490	13	8.7	1.7	101649
685[O]	2496	13	8.0	1.7	101650
684[O]	2503	17	6.9	2.2	103365
683[O]	2500	16	7.1	2.1	104462
682[O]	2493	13	7.9	1.6	102850
681[O]	2479	12	9.6	1.6	104461
680[O]	2529	17	3.2	2.2	100864
680[O]	2510	13	5.6	1.6	100865
679[O]	2495	13	7.4	1.6	104460
678[O]	2515	17	4.7	2.1	103348
677[O]	2483	15	8.5	1.9	104458
676[O]	2500	18	6.3	2.3	103366
675[O]	2521	12	3.6	1.5	102851
675[O]	2525	11	3.0	1.4	102852
674[O]	2508	13	5.1	1.6	104457
673[O]	2510	13	4.7	1.6	104456
672[O]	2530	18	2.2	2.2	103349
671[O]	2488	15	7.2	1.9	104455
670[P, O]	2481	14	8.0	1.8	101647
670[P, O]	2496	15	6.1	1.9	101648
669[P, O]	2492	14	6.5	1.7	104454
668[P, O]	2508	17	4.4	2.2	103367
667[P, O]	2504	17	4.7	2.1	103350
666[P, O]	2518	12	2.8	1.6	104453
665[P, O]	2491	14	6.2	1.7	101645
665[P, O]	2468	16	9.0	2.0	101646
664[P, O]	2479	17	7.5	2.1	103368
663[P, O]	2470	14	8.5	1.8	104452
662[P, O]	2441	19	12.1	2.4	103351
661[P, O]	2447	12	11.2	1.6	104451
660[P, O]	2407	14	16.1	1.8	101643
660[P, O]	2416	14	14.9	1.7	101644
659[P, O]	2430	13	13.0	1.6	104450
658[P, O]	2442	17	11.4	2.1	103369
657[P, O]	2444	17	11.0	2.2	103370
656[P, O]	2458	12	9.2	1.6	104449
655[P, O]	2437	13	11.7	1.6	102853
654[P, O]	2437	17	11.6	2.2	103371
653[P, O]	2467	13	7.7	1.6	104448
652[P, O]	2472	17	6.9	2.1	103352
651[P, O]	2474	13	6.6	1.6	104447
650[O]	2452	12	9.2	1.5	102854

https://doi.org/10.1017/RDC.2020.16 Published online by Cambridge University Press

Table 3 (*Continued*)

Year (yr BC)	^{14}C age (yr BP)	^{14}C age error (yr BP)	Δ^{14}C (‰)	Δ^{14}C error (‰)	UCIAMS #
649^{O}	2465	17	7.4	2.1	103372
648^{O}	2476	13	5.9	1.6	104446
647^{O}	2454	18	8.6	2.2	103353
646^{O}	2470	13	6.4	1.6	104445
645^{O}	2461	13	7.4	1.7	101641
645^{O}	2479	14	5.2	1.7	101642
644^{O}	2483	17	4.6	2.1	103373
643^{O}	2489	13	3.7	1.6	104444
642^{O}	2489	18	3.6	2.3	103354
641^{O}	2500	13	2.0	1.6	104443
640^{O}	2477	13	4.9	1.6	102855
639^{O}	2497	17	2.2	2.1	103374
638^{O}	2482	15	3.9	1.9	104442
637^{O}	2482	17	3.9	2.1	103355
636^{O}	2483	17	3.6	2.1	103375
635^{O}	2472	12	4.9	1.5	104441
634^{O}	2501	14	1.1	1.7	100866
634^{O}	2491	13	2.4	1.6	100867
633^{O}	2516	17	–0.8	2.1	103376
632^{O}	2504	17	0.4	2.1	103356
631	2495	13	1.5	1.6	104440
630	2491	11	1.9	1.4	102856
629	2488	19	2.1	2.4	103377
628	2503	13	0.1	1.6	104439
627	2523	13	–2.5	1.6	104438
626	2515	15	–1.6	1.9	104437

Table 4 Single-year dates from the White Mountains, California, CAM 143, whole-year rings. Alternative dendro dates (due to year 0 problem) are indicated in parentheses.

Year (yr BC)	^{14}C age (yr BP)	^{14}C age error (yr BP)	Δ^{14}C (‰)	Δ^{14}C error (‰)	UCIAMS #
661 (662?)	2452	17	10.5	2.1	100572
662 (663?)	2438	16	12.4	2.0	100573
663 (664?)	2464	16	9.3	2.0	100574
664 (665?)	2484	18	6.9	2.3	100575
665 (666?)	2519	16	2.6	2.0	100576
666 (667?)	2502	18	4.9	2.3	100577
667 (668?)	2501	17	5.1	2.1	100578
668 (669?)	2499	17	5.5	2.1	100579
669 (670?)	2499	16	5.6	2.0	100580

https://doi.org/10.1017/RDC.2020.16 Published online by Cambridge University Press

670 (671?)	2501	17	5.5	2.1	100581
671 (672?)	2506	17	5.0	2.1	100582
672 (673?)	2529	17	2.2	2.1	100583
673 (674?)	2511	18	4.6	2.3	100584
674 (675?)	2501	16	6.0	2.0	100585
675 (676?)	2522	16	3.5	2.0	100586
676 (677?)	2528	17	2.8	2.1	100587
677 (678?)	2537	18	1.8	2.2	100588
678 (679?)	2532	17	2.6	2.1	100589
679 (680?)	2489	16	8.1	2.0	100590
680 (681?)	2510	17	5.6	2.1	100591
681 (682?)	2528	13	3.4	1.6	101348
682 (683?)	2511	13	5.7	1.6	101349
683 (684?)	2501	13	7.1	1.6	101350
684 (685?)	2515	15	5.4	1.9	101351
685 (686?)	2521	13	4.8	1.6	101352
686 (687?)	2506	13	6.8	1.6	101353
687 (688?)	2485	13	9.6	1.6	101354
688 (689?)	2508	14	6.8	1.8	101355
690 (691?)	2509	13	6.9	1.6	101356
691 (692?)	2463	14	12.8	1.8	101357

https://doi.org/10.1017/RDC.2020.16 Published online by Cambridge University Press